UNCLASSIFIED

AD 297 244

Reproduced
by the

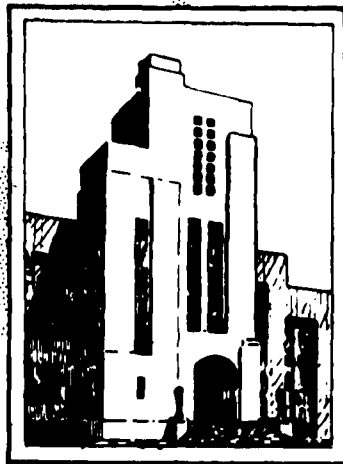ARMED SERVICES TECHNICAL INFORMATION AGENCY
ARLINGTON HALL STATION
ARLINGTON 12, VIRGINIA

UNCLASSIFIED

HYDROMECHANICS

○

AERODYNAMICS

○

STRUCTURAL
MECHANICS

○

APPLIED
MATHEMATICS

DEPARTMENT OF THE NAVY
DAVID TAYLOR MODEL BASIN

INVESTIGATION OF THE INFLUENCE OF STIFFENER
SIZE ON THE BUCKLING PRESSURES
OF CIRCULAR CYLINDRICAL SHELLS
UNDER HYDROSTATIC PRESSURE,
PART II

by

James A. Nott

STRUCTURAL MECHANICS LABORATORY
RESEARCH AND DEVELOPMENT REPORT

INVESTIGATION OF THE INFLUENCE OF STIFFENER SIZE ON THE BUCKLING PRESSURES OF CIRCULAR CYLINDRICAL SHELLS UNDER HYDROSTATIC PRESSURE, PART II

by

James A. Nott

The present report summarizes the detailed theoretical and experimental analyses presented in the two previous manuscripts, and also, discusses the comparison between the theoretical analysis of this report and a later analysis developed by Doctor G. Gerard.

January 1963   Report 1688

Investigation on the Influence of Stiffener Size on the Buckling Pressures of Circular Cylindrical Shells Under Hydrostatic Pressure[1]

By James A. Nott[2]

A theoretical derivation is given for elastic and plastic buckling of stiffened, circular cylindrical shells under uniform external hydrostatic pressures. The theory accounts for variable shell stresses, as influenced by the circular stiffeners, and critical buckling pressures are obtained for simple support conditions at the shell-frame junctures. Collapse pressures for both elastic and plastic buckling are determined by iteration and numerical minimization. The theory is applicable to shells made either of strain-hardening or elastic-perfectly plastic materials. Using the developed analysis, it is shown that a variation in stiffener size can change the buckling pressures. Test data from high-strength steel and aluminum cylinders show agreement between the theoretical and experimental collapse pressures to within approximately six percent.

SINCE the USS *Holland* was launched, the Navy has been interested in the design of reinforced cylinders for submarine structures. Collapse pressures for various modes of failure must be determined before the naval architect can arrive at a rational design. The collapse of a cylindrical shell stiffened by circular frames may occur in one of three modes depending upon its geometry. Considering a given shell-thickness to shell-diameter ratio, failure may occur by

1 General instability.
2 Asymmetric shell buckling.
3 Or axisymmetric shell collapse.

General instability occurs when the size of the frames is critical for a given frame spacing, resulting in collapse of the frames together with the shell. Failure may occur along several frames or it may occur over the entire length of a compartment. Shell buckling occurs when frame size is sufficient to prevent general instability, but the frame spacing is critical. In this type of shell failure a series of asymmetric lobes forms in the shell between frames. Axisymmetric shell collapse occurs when the frame size is sufficient to prevent general instability and

Nomenclature

A_F = effective area of frame cross section, sq in.
A_i = coefficients for plastic-buckling equation, in.$^{-4}$
b = faying width of frame, in.
D = bending rigidity of shell, $E_s h^3/12(1 - \nu^2)$, lb-in.
E = Young's modulus, psi
E_s = secant modulus, psi
E_t = tangent modulus, psi
h = shell thickness, in.
k = mode shape coefficient, n/R, in.$^{-1}$
l_F = center-to-center spacing of frames, in.
L = unsupported length of cylinder, $l_F - b$, in.
M = moduli parameter, $1 - E_t/E_s$, dimensionless
m, n = numbers of half-waves of buckling configuration in axial and circumferential directions, respectively, dimensionless
$N_x, N_\theta, N_{x\theta}$ = forces per unit length, lb per in.
p = pressure, psi
p_e = elastic buckling pressure, psi
p_p = plastic buckling pressure, equation (10), psi
p_c = plastic collapse pressure, equations (10) and (13), psi

R = radius of cylinder to midplane of shell, in.
R_F = radius of cylinder, to CG of frame, in.
u, v, w = shell displacements, in.
x, y, z = coordinates, dimensionless
α = effective stress parameter, $3(1 - E_t/E_s)/\sigma_i{}^2$
γ_1 = measure of beam-column effect, $(R/h)^3 p/2E (1 - \nu^2)^{1/2}$ dimensionless
ξ = property parameter, $\dfrac{h/R}{\sigma_y/E}$, dimensionless
θ = shell flexibility parameter, $[3(1 - \nu^2)]^{1/4} L/(R h)^{1/2}$, dimensionless
λ = mode shape coefficient, $m\pi/L$, in.$^{-1}$
ν = Poisson's ratio, dimensionless
ν_e = elastic value of Poisson's ratio, dimensionless
σ_x, σ_θ = membrane stresses, psi
σ_i = effective stress, psi
σ_e = elastic limit stress, psi
σ_y = yield stress, psi
ϕ = stress function, dimensionless
τ = shear stress, psi

the frame spacing-diameter ratio is relatively small, preventing shell buckling. Failure occurs by a combination of yielding and axisymmetric buckling of the shell, resulting in an axisymmetric fold in the shell between frames.

Theoretical solutions for the elastic instability of cylindrical shells have been derived by Mises [1] and Sanden and Tölke [2], and their solutions apply when stresses in the shell are linear when buckling occurs. The problem of plastic collapse has been recently treated by Reynolds [3] for the asymmetric mode of failure and by Lunchick [4, 5] for the axisymmetric mode. In their solutions the nonlinear effect of the stress-strain curve in the elastic-plastic region is considered.

A subject of current interest to the naval architect is that of the effect of the size of the reinforcing circular frames on the asymmetric shell-buckling strength of cylindrical shells under external hydrostatic pressure. This problem becomes important in the design of submarines, since it is advantageous to have the structural material in the shell and frame so distributed that it gives a maximum collapse pressure for a minimum weight.

In this report a theoretical analysis of the asymmetric shell-buckling mode of a circular, framed, cylindrical shell loaded under external uniform hydrostatic pressure is shown. Gerard's [6] equations of equilibrium for plastic buckling are solved using realistic expressions for stresses in the shell determined by the Salerno-Pulos [7] theory, which accounts for the effect of circular frames. The plasticity coefficients in Gerard's equations of equilibrium are expressed in terms of variable shell stresses determined by Salerno and Pulos. The feature of variable shell stresses becomes important in this problem, as a change in frame size will produce a change in shell stresses.

Theory

Plastic-Buckling Theory

In the case of stiffened circular cylindrical shells loaded under external hydrostatic pressure the two principal stresses occur in directions parallel and perpendicular to the longitudinal axis of the cylinder, Fig. 1. Therefore, the shear stress is given by

$$\tau = \frac{N_{rt}}{h} = 0 \tag{1}$$

Using membrane-stress theory, which considers only stresses on the middle surface of the shell (neglecting bending), the longitudinal membrane stress can be determined from the equation of equilibrium in the longitudinal direction:

$$\sigma_t = \frac{N_t}{h} = \frac{pR}{2h} \tag{2}$$

The circumferential membrane stress can be obtained by the analysis of Salerno and Pulos [7] who express the stress as follows:

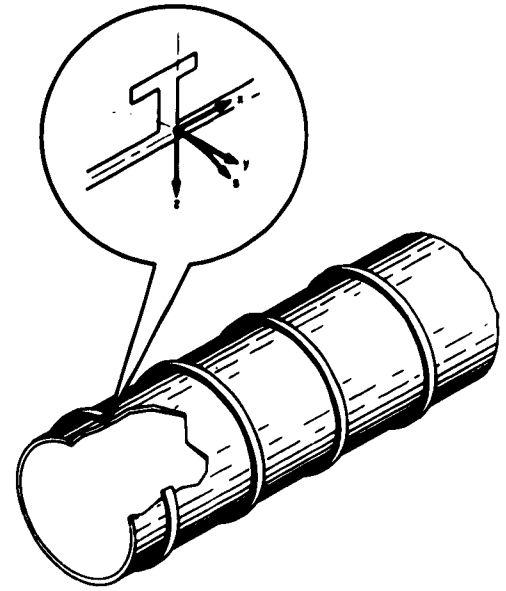¹ Numbers in brackets designate References at end of paper.

Fig. 1 Coordinate system for stiffened cylindrical shell

$$\sigma_t = \phi \frac{pR}{h} \tag{3}$$

where

$$\phi = \phi(p)$$

In the theory of buckling, a certain stress condition at a point in the shell is assumed to reach a limiting value at the onset of collapse. The circumferential stress varies with x and the stress condition is assumed to be most critical at midbay; therefore, the stress is taken at the midbay, midplane fiber location. The function, ϕ, which determines the axisymmetric stress at this location of a circular framed cylindrical shell loaded under external hydrostatic pressure is given by the theory of Salerno and Pulos [7] and expressed by Krenzke and Short [8] in the following convenient form:

$$\phi = 1 - \frac{\left(1 - \frac{\nu}{2}\right) \alpha_1 F_2}{\alpha_1 + \beta + F_1(1 - \beta)} \tag{4}$$

where α_1 is the ratio of frame area to shell area and is expressed as

$$\alpha_1 = \frac{A_F}{hL_F} \tag{4a}$$[4]

and β is the ratio of faying width of the stiffener to the center-to-center spacing of the stiffeners and is expressed as

$$\beta = \frac{b}{L_F} \tag{4b}$$

The functions F_1 and F_2 are defined as follows:

$$F_1 = \binom{4}{\theta}\left[\frac{\cosh^2 \eta_1\theta - \cos^2 \eta_2\theta}{\dfrac{\cosh \eta_1\theta \sinh \eta_1\theta}{\eta_1} + \dfrac{\cos \eta_2\theta \sin \eta_2\theta}{\eta_2}}\right] \quad (4c)$$

$$F_2 = \frac{\dfrac{\cosh \eta_1\theta \sin \eta_2\theta}{\eta_2} + \dfrac{\sinh \eta_1\theta \cos \eta_2\theta}{\eta_1}}{\dfrac{\cosh \eta_1\theta \sinh \eta_1\theta}{\eta_1} + \dfrac{\cos \eta_2\theta \sin \eta_2\theta}{\eta_2}}$$

where

$$\eta_1 = \tfrac{1}{2}(1 - \gamma_1)^{1/2} \text{ and } \eta_2 = \tfrac{1}{2}(1 + \gamma_1)^{1/2}$$

Gerard's [6] equilibrium equations for cylindrical-shell structures made of an isotropic, incompressible material and subjected to external hydrostatic pressure can be written in terms of the shell stresses, σ_z and σ_s, as follows:

$$\left(1 - \alpha\frac{\sigma_z^2}{4}\right)\frac{\partial^2 u}{\partial x^2} + \frac{1}{4}\frac{\partial^2 u}{\partial s^2} + \left(\frac{3}{4} - \alpha\frac{\sigma_z\sigma_s}{4}\right)\frac{\partial^2 v}{\partial x\partial s}$$
$$+ \left(\frac{1}{2} - \alpha\frac{\sigma_z\sigma_s}{4}\right)\frac{1}{R}\frac{\partial w}{\partial x} = 0$$

$$\left(1 - \alpha\frac{\sigma_s^2}{4}\right)\frac{\partial^2 v}{\partial s^2} + \frac{1}{4}\frac{\partial^2 v}{\partial x^2} + \left(\frac{3}{4} - \alpha\frac{\sigma_z\sigma_s}{4}\right)\frac{\partial^2 u}{\partial x\partial s}$$
$$+ \left(1 - \alpha\frac{\sigma_s^2}{4}\right)\frac{1}{R}\frac{\partial w}{\partial s} = 0$$

$$(5)$$

$$D\left[\left(1 - \alpha\frac{\sigma_z^2}{4}\right)\frac{\partial^4 w}{\partial x^4} + \left(2 - \alpha\frac{\sigma_z\sigma_s}{2}\right)\frac{\partial^4 w}{\partial x^2\partial s^2}\right.$$
$$+ \left(1 - \alpha\frac{\sigma_s^2}{4}\right)\frac{\partial^4 w}{\partial s^4}\right] + \frac{4E_s h}{3R}\left[\left(\frac{1}{2} - \alpha\frac{\sigma_z\sigma_s}{4}\right)\frac{\partial u}{\partial x}\right.$$
$$+ \left.\left(1 - \alpha\frac{\sigma_s^2}{4}\right)\left(\frac{\partial v}{\partial s} + \frac{w}{R}\right)\right] + N_z\frac{\partial^2 w}{\partial x^2}$$
$$+ N_s\frac{\partial^2 w}{\partial s^2} + p = 0$$

where

$$\alpha = \frac{3}{\sigma_i^2}\left(1 - \frac{E_t}{E_s}\right)$$

in which the effective stress, σ_i, is determined from the octahedral shear-stress theory of Hencky, Huber, and Mises; i.e.,

$$\sigma_i = (\sigma_z^2 + \sigma_s^2 - \sigma_z\sigma_s)^{1/2} \quad (6)$$

If simple support conditions are assumed at the shell-frame junctures, the boundary conditions which must be satisfied are

$$w|_{x=0} = w|_{x=L} = 0 \quad (7)$$

and

$$\frac{\partial^2 w}{\partial x^2}\bigg|_{x=0} = \frac{\partial^2 w}{\partial x^2}\bigg|_{x=L} = 0 \quad (8)$$

Simple support implies that the frames offer no restraint

to longitudinal bending in the shell at the shell-frame junctures. This assumption at the boundary may be justified by concluding that, when plastic behavior begins in the shell at the shell-frame junctures, the frames produce little restraint against rotation of the shell. The general solution of equations [5] satisfying the boundary conditions, equations (7) and (8), can be expressed as

$$\begin{aligned} u &= A_0 \sin ks \cos \lambda x \\ v &= B_0 \cos ks \sin \lambda x \\ w &= C_0 \sin ks \sin \lambda x \end{aligned} \quad (9)$$

In small-displacement theory, the criterion for bifurcation of equilibrium is that the deflections increase beyond limit. To satisfy this stability criterion, the expressions for the displacements, u, v, and w, given by equations (9), are substituted into the equilibrium equations, equations (5), and the determinant formed by the coefficients of the arbitrary mode-shape parameters, A_0, B_0, and C_0, is set equal to zero. Equating this determinant to zero, a characteristic equation for the determination of the plastic-buckling pressure is obtained. The method of solution is shown in detail by Nott in [9]. The plastic buckling pressure is expressed in the form

$$p_s = \frac{4D[A_1 - (CM)x_1 + (CM)^2 x_2] + \dfrac{E_s h\lambda^4}{R^2}}{R\left(\dfrac{\lambda^2}{2} + k^2\phi\right)\left\{(k^2 + \lambda^2)^2 - M\right.}$$
$$\left[4C\left(\dfrac{\lambda^2}{2} - k^2\phi\right)^2 + 3\lambda^2 k^2\right]\right\} \quad (10)$$

where

$$C = \frac{3}{4(4\phi^2 - 2\phi + 1)} \quad (10a)$$

$$M = 1 - \frac{E_t}{E_s} \quad (10b)$$

$$\begin{aligned} x_1 &= A_2 - A_3\phi + A_4\phi^2 \\ x_2 &= A_5 + A_6\phi + A_7\phi^2 - A_8\phi^3 + A_9\phi^4 \end{aligned} \quad (10c)$$

and

$$\begin{aligned} A_1 &= \tfrac{1}{4}(k^2 + \lambda^2)^4 \\ A_2 &= \tfrac{1}{4}\lambda^2(k^2 + \lambda^2)^2(2k^2 + \lambda^2) \\ A_3 &= 2k^2\lambda^2(k^2 + \lambda^2)^2 \\ A_4 &= 2k^2(k^2 + \lambda^2)^2(k^2 + 2\lambda^2) \\ A_5 &= \tfrac{1}{4}\lambda^6(4k^2 + \lambda^2) \\ A_6 &= 2k^2\lambda^4(2k^2 - \lambda^2) \\ A_7 &= 2k^2\lambda^2(2k^2 - \lambda^2)(k^2 - 2\lambda^2) \\ A_8 &= 8k^4\lambda^2(k^2 - 2\lambda^2) \\ A_9 &= 4k^6(k^2 + 4\lambda^2) \end{aligned} \quad (10d)$$

Equation (10) is an exact solution for the case of simple support conditions at the shell-frame junctures. Gerard, in [10], obtains an approximate plasticity reduction factor for asymmetric buckling. In his solution, Gerard makes the assumption that

$$\left(\frac{nL}{\pi R}\right)^2 \gg 1$$

This assumption for "moderate length cylinders" leads to neglecting of higher order terms which enables an analytical minimisation of the plasticity equations. However, in the general case of cylinders of any length no assumption can be made as to the order of magnitude of $nL/\pi R$. Hence, the expression for the critical pressure becomes more complicated, and the minimisation with respect to the number of lobes (n) is not as convenient as in Gerard's case.

The plastic-buckling pressure, p_p, in equation (10) defines a range of collapse pressures for different values of σ_i beyond the elastic limit. The flexural rigidity of the shell, D, in equation (10) is given by

$$D = \frac{E_t h^3}{12(1 - \nu^2)} \tag{11}$$

where Poisson's ratio, ν, in the elastic-plastic region is shown by Gerard and Wildhorn [11] to be

$$\nu = \frac{1}{2} - \frac{E_t}{E}\left(\frac{1}{2} - \nu_e\right)^{\cdot} \tag{12}$$

Equation (6) can also be used to determine the relationship between the prebuckling stress condition in the shell and the applied pressure. Substituting equations (2) and (3) into equation (6) and solving for p, one obtains

$$p_i = \frac{2h\sigma_i}{R(4\phi^2 - 2\phi + 1)^{1/2}} \tag{13}$$

Since ϕ is a function of the applied pressure, equations (10) and (13) represent transcendental equations for the pressures p_p and p_i, respectively.

Buckling of a cylindrical shell in the asymmetric mode is assumed to occur when the applied pressure, p_i, equals the plastic-buckling pressure, p_p. Therefore, the plastic-collapse pressure, p_c, which uniquely defines the plastic-buckling pressure of the shell, is obtained by the simultaneous solution of equations (10) and (13). As an analytical solution to these equations would be quite tedious, if not impossible, a graphical solution is recommended. Equation (10) can be plotted in the form p_p versus σ_i and equation (13) in the form p_i versus σ_i. The intersection of these two curves then defines the collapse pressure, p_c.

Minimum or critical values of p_p in the elastic-plastic region for a specific geometry are determined by: (a) Numerical minimisation with respect to n, and (b) an iteration procedure to satisfy equations (4) and (10). Iteration is also used to determine p_i from equations (4) and (13). This procedure, outlined for a strain-hardening material, is greatly simplified for an elastic-perfectly plastic material. As the value of σ_i for an elastic-perfectly plastic material is never greater than σ_y, equation (10) represents the vertical line $\sigma_i = \sigma_y$.

Elastic-Buckling Theory

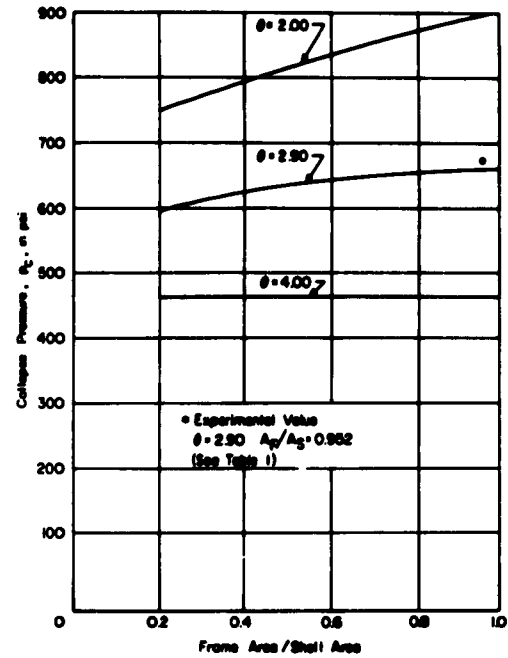When the geometry of the shell structure is such that elastic buckling can occur, the intersection of p_p versus

Fig. 2 Effect of frame size on shell-buckling pressures of steel cylinders

σ_i and p_i versus σ_i occurs for a value of σ_i less than σ_e, the elastic limit of the material. In this case $E_t/E_e = 1$ and equation (10) reduces to Reynolds [3] elastic-buckling pressure, p_e, which can be written as

$$p_e = \frac{Eh}{R}\left[\frac{\dfrac{h^2(k^2 + \lambda^2)^2}{12(1 - \nu_e^2)} + \dfrac{\lambda^4}{R^2(k^2 + \lambda^2)^2}}{\dfrac{\lambda^2}{2} + k^2\phi}\right] \tag{14}$$

A plot of p_e versus σ_i is the horizontal line $p = p_e$ in the $p - \sigma_i$ plane and, therefore, the critical buckling pressure may be obtained directly from equation (14). Equation (14) is also a transcendental equation in the pressure, and the elastic-collapse pressure, p_e, must be determined by iteration.

Theoretical Results

Calculations have been carried out for a series of geometries in the plastic-buckling range to show the effect of frame size on the shell-buckling pressure, p_c, according to the developed theory. A strain-hardening steel with a yield strength of 88,000 psi is used for demonstration purposes, and the results are presented in graphical form in Fig. 2. As shown in the graph, the flexibility parameter, θ, has a limiting value of 4.0, for which an increase of the relative frame size will not produce any increase in collapse pressure. Thus, at this limit the ratio of frame area to shell area need only be sufficient to prevent combined frame and shell failure. Since θ is a function of h and R and is directly propor-
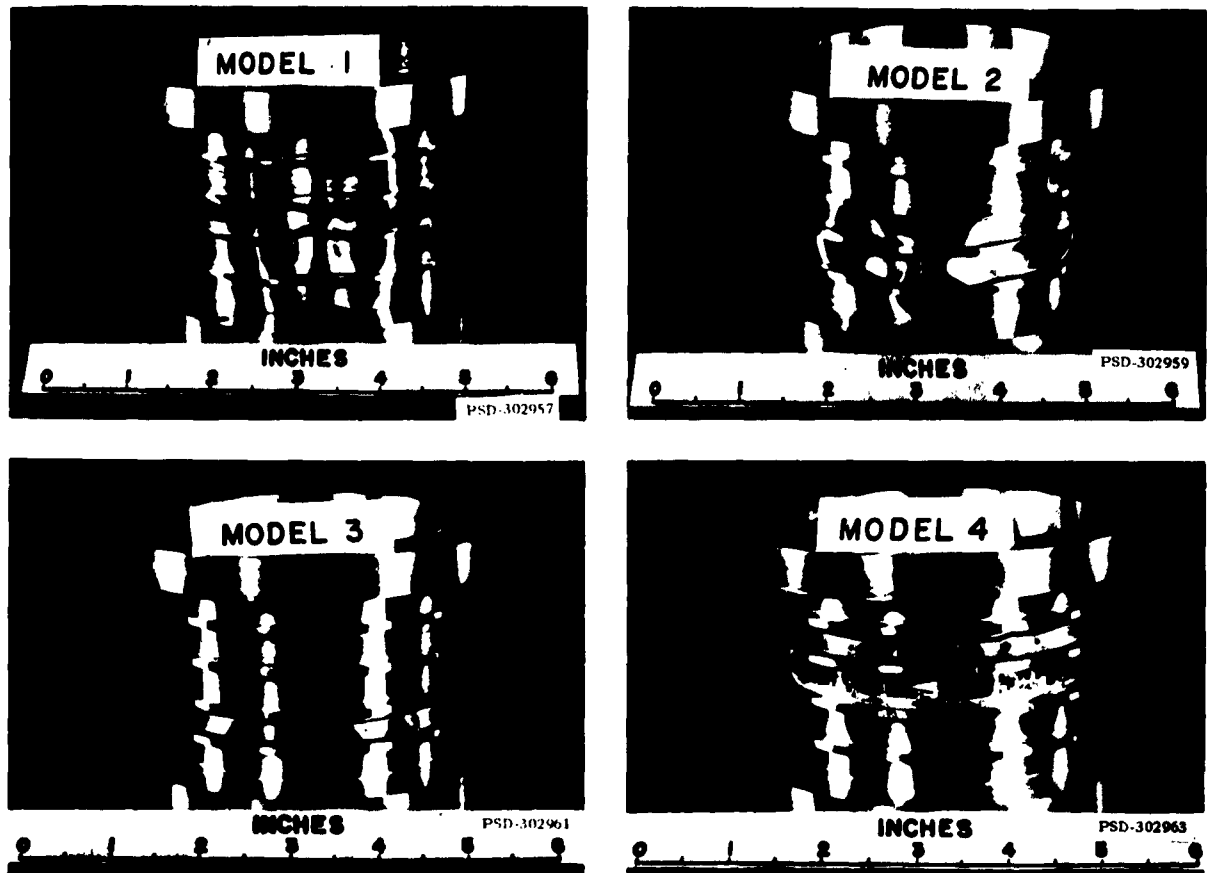
4

Fig. 3 Aluminum models after collapse

tional to the spacing, L, it is seen that for a constant h and R, θ is totally dependent on L. For this case, frame spacing is an important aspect on the effect of frame size.

Experiment

Description of Models

To determine experimentally what effect the circular frames have on a cylindrical shell loaded under external hydrostatic pressure, four structural models were fabricated and tested in a pressure tank. As pioneering structural research is currently being conducted in the use of aluminum for oceanographic research vehicles, for example, the *Aluminaut*, a high-strength aluminum alloy was chosen. The four models were constructed of 7075-T6 extruded aluminum. Machined structural models were favored as opposed to welded models to eliminate the effects of initial deflections and residual stresses which occur in welded structures. Lunchick and Short [12] and Krenzke [13] have shown that, in welded models, the heating and cooling process occurring when the webs of the frames are welded to the shell causes an initial outward shell deflection for an externally-framed cylinder. On the other hand, an initial inward shell deflection occurs for an internally-framed cylinder. These initial deflections cause residual stresses and beam-column effects which can affect the collapse strength.

Each model had the same shell thickness, radius, and typical bay lengths, and only the cross-sectional area of the frames varied. The shell flexibility parameter, θ, was 2.5 for each model.

Model 1 had a frame area equal to 30 percent of the shell area. The frame area of Model 2 was 40 percent of that in the shell. Model 3 had a frame area 70 percent of the shell, and Model 4, 100 percent of the shell area. The shape of the frames on all four models was that of a T-section, and the faying width of the webs was held constant in order to hold the bay lengths the same.

Test Results

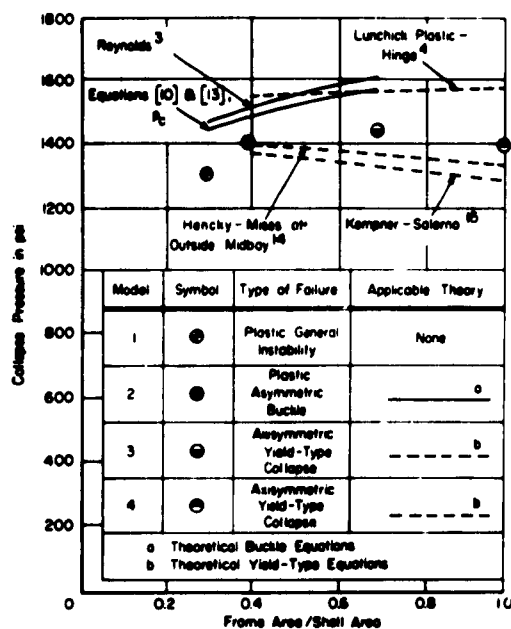Fig. 3 shows the four models after collapse. Model 1, which had a cross-sectional frame area 30 percent of the

Fig. 4 Effect of frame size on collapse pressures of aluminum cylinders

Fig. 5 Effect of frame size on axisymmetric strains of aluminum cylinders

shell area, collapsed at a pressure of 1300 psi by plastic general instability. The frames were not of sufficient size to prevent frame failure, and both frames and shell failed simultaneously over the entire length of the model in a single "deep dish" lobe. Width of the lobe was approximately one eighth of the circumference of the model. Tearing of the shell from the end rings and frames occurred throughout the lobe, and the two center frames buckled inward.

Model 2, which had a cross-sectional frame area 40 percent of the shell area, collapsed at 1400 psi by plastic asymmetric buckling. Failure occurred in all three typical bays in a series of nonsymmetrical lobes accompanied by lateral twisting of the frames. The length of the lobes was approximately one tenth of the circumference of the model. In several places tearing occurred at the shell-frame junctures, but this was not as pronounced as in Model 1.

Model 3, which had a cross-sectional frame area 70 percent of the shell area, collapsed at 1420 psi by axisymmetric shell yielding. Failure occurred in the first typical bay from the end ring along a 180-deg arc length around the circumference. Tearing occurred at the two shell-frame junctures and at midbay.

Model 4, which had a cross-sectional frame area 100 percent of the shell area, collapsed at 1390 psi by axisymmetric shell yielding similar to Model 3; however, the area of collapse was more pronounced in Model 4. The length of the failure in this model extended over approximately 200 deg. Failure occurred in the first typical bay from the end ring and tearing of the shell at the hinge locations occurred as in Model 3.
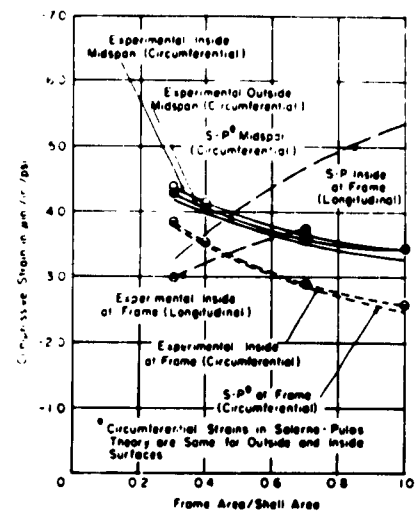
A graphical representation of the observed collapse pressures is shown in Fig. 4, together with various corresponding theoretical formulas. The Hencky-Mises [14] yield criterion at outside midbay assumes that failure occurs when the effective stress, σ_i, on an outside fiber at midbay reaches the yield strength of the material. An extension of this theory is that of Kempner and Salerno [15], in which failure is assumed to occur when the stresses inside at the frame, followed by stresses at outside midbay, reach the yield strength. Lunchick's plastic-hinge theory [4] for axisymmetric collapse is for an elastic-perfectly plastic material and allows for an amount of plastic reserve strength before failure occurs.

Discussion of Experimental Results

The experimental results showed that an appreciable increase in collapse pressure occurred from the 30 percent frame-area case to the 40 percent frame-area case. At the 30 percent frame area a general instability failure occurred. At the 40 percent frame area buckling of the shell occurred between frames. Only a small increase in collapse pressure occurred between 40 percent and 70 percent frame size. At 70 percent frame size an axisymmetric yield-type failure occurred instead of asymmetric buckling. Strains at the frame indicated that longitudinal stresses grow with an increase of percent frame size, Fig. 5, which could cause premature yielding. A subsequent increase to 100 percent frame size caused collapse at a lower pressure than that of the 40 percent frame size. For an increase in percent frame size, the relative decrease in circumferential strains at a frame was greater than the decrease in circumferential strains at midbay. This shows that large frames lower frame deflections, but increase bending of the shell at the frames, thus causing relatively higher longitudinal stresses in the shell at the frame locations. Therefore, in the case of the 100 per-

Table I Comparison of Theoretical Versus Experimental Collapse Pressures

Model Number	T-2	T-3	T-6	T-2A	T-7A	U-12	U-22	2
Frame Area/Shell Area	0.952	0.694	0.609	0.418	0.209	0.488	0.576	0.400
$\sigma_y/E \times 10^3$	2.93	3.00	3.03	3.43	2.00	2.27	2.35	6.09
$h/R \times 10^2$	0.679	0.669	0.953	0.653	0.979	1.093	0.873	1.525
Shape of Frame	Tee					Rectangular		Tee
Material	T-Steel					Mild Steel		7075-T6
Construction	Welded					Machined		
Experimental Collapse Pressure (psi)	670	553	1005	600	770	975	735	1400
Plastic Buckling — Equations (10) and (13), p_c	662	548	980	691	743	917	707	1485
Plastic Buckling — Reynolds[3]	696	563	1016	705	748	938	734	1502
Elastic Buckling — Equation (14), p_o	878	603	1210	755	978	1895	988	1943
Elastic Buckling — Reynolds[3]	906	626	1259	756	1010	1907	1002	1976
Elastic Buckling — Sanden-Tolke[2]	930	631	1258	773	1032	2014	1054	1977
Elastic Buckling — Mises[1]	786	585	1190	705	995	1786	963	1815

cent frame size, the bending stresses in the shell at the frames could have affected the collapse pressure adversely.

Comparison of Theory With Experiment

For the models tested, the asymmetric theory predicts an increase in shell-buckling pressure for an increase in frame size. Since only Model 2 failed in this mode, it is difficult to make a positive conclusion concerning the actual trend. However, it would seem reasonable to assume, from the much lower collapse pressure of Model 1 and the higher pressure of Model 3, that the experimental buckling pressures also increase with an increase of frame size to a point where axisymmetric collapse occurs. This increase in buckling pressure for an increase of frame size agrees with equations (10) and (13) as shown in Fig. 4. Using equations (10) and (13) and Lunchick's plastic-hinge theory [4] for axisymmetric collapse, the transition between asymmetric and axisymmetric collapse occurs for a frame area 62 percent of the shell area, which case is between Models 2 and 3.

The solution of equations (10) and (13) of this report, Reynolds' theory [3], and Lunchick's plastic-hinge theory [4] all predict collapse pressures on the unconservative side of the experimental values. Reynolds does not completely account for actual prebuckling stresses in the shell as influenced by the frames, and the plastic-hinge theory is not strictly applicable to a strain-hardening material.

When the Hencky-Mises yield criterion [14] is applied to the stresses at the outside midbay location, theoretical collapse pressures are on the conservative side of the experimental values. The theory of Kempner and Salerno [15] shows collapse pressures slighty lower than those given by the Hencky-Mises criterion.

Reynolds [3], in his comprehensive study of plastic buckling, also reported the test results of seven steel models, five of welded construction and two machined. Results of these tests and results of Model 2 are compared with theoretical formulae in Table 1. Fig. 6 gives a graphical representation of theoretical versus experimental collapse pressures for the steel cylinders shown in Table 1. Equations (10) and (13) and Reynolds' plastic equations are shown to agree within approximately 6 percent of experiments. The elastic equations, equation (14), and those of Mises [1], Sanden and Tölke [2], and Reynolds [3], predict collapse pressures which are unconservative when compared with the experimental results. This can be expected, since all the test models collapsed plastically.

A property parameter, defined

$$\xi = \frac{h/R}{\sigma_v/E} \tag{15}$$

is shown superimposed on the graphs in Fig. 6. When h/R is relatively high and σ_v/E is relatively small, a high value of ξ is obtained. This is the case for Model U-12, in which h/R is 0.0193 and σ_v/E is 2.27×10^{-3} for 0.488 frame-area to shell-area ratio, Table 1. Also, for small values of h/R and large σ_v/E a low ξ is obtained, as is the case for Models T-2A and T-3. The trend of the ξ-curve in Fig. 6 agrees with the trend of the elastic-buckling equations. This should be expected, since for Model U-12 the large h/R increases the theoretical elastic-
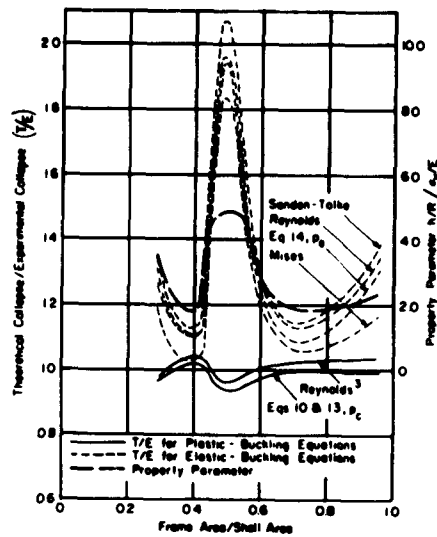
Fig. 6 Graphical comparison of theoretical versus experimental collapse pressures for steel cylinders

buckling pressure, and the small σ_y/E lowers the experimental collapse pressure. Thus, for this case, a high ratio of theoretical collapse to experimental collapse is obtained. Conversely, for Models T-2A and T-3 the small h/R and large σ_y/E produce more conservative values for the ratio of theoretical collapse to experimental collapse.

Conclusions

The following conclusions can be made for stiffened cylindrical shells loaded under external hydrostatic pressure:

1 The theory presented by the author for asymmetric buckling adequately predicts collapse pressures for shell geometries constructed from (a) high-strength steel, and (b) high-strength aluminum, when the observed collapse is in the asymmetric mode.

2 A decrease in the shell flexibility parameter, θ, leads to:

(a) An increase in the plastic asymmetric buckling pressures, p_c, for a specified percent frame size.

(b) A higher rate of increase in the plastic buckling pressures for an increase in percent frame size.

3 For a cylinder made of 7075-T6 aluminum and having a shell flexibility parameter of 2.5, an increase in relative frame size leads to:

(a) A change in the observed mode of failure between 30 percent and 40 percent frame size from plastic general instability to plastic asymmetric buckling.

(b) A change in the observed mode of failure between 40 percent and 70 percent frame size from plastic buckling to an axisymmetric yield-type collapse.

(c) A change in the predicted mode of failure from asymmetric buckling to axisymmetric yielding at 62 percent frame size; Lunchick's [4] plastic hinge and equations (10) and (13), p_c.

(d) An increase in the theoretical asymmetric buckling pressures between 30 and 70 percent frame size.

(e) An increase in the experimental and theoretical longitudinal bending strains at the frame locations.

(f) A decrease in the experimental and theoretical circumferential strains at the midbay and frame locations.

References

1 R. Von Mises, "The Critical External Pressure of Cylindrical Tubes Under Uniform Radial and Axial Load," Experimental Model Basin Translation 366, August, 1933.

2 K. Von Sanden, and F. Tölke, "On Stability Problems in Thin Cylindrical Shells," David Taylor Model Basin Translation 33, December, 1949.

3 T. E. Reynolds, "Inelastic Lobar Buckling of Circular Cylindrical Shells Under External Hydrostatic Pressure," David Taylor Model Basin Report 1392, August, 1960.

4 M. E. Lunchick, "Yield Failure of Stiffened Cylinders Under Hydrostatic Pressure," David Taylor Model Basin Report 1291, January, 1959.

5 M. E. Lunchick, "Plastic Axisymmetric Buckling of Ring-Stiffened Cylindrical Shells Fabricated From Strain-Hardening Materials and Subjected to External Hydrostatic Pressure," David Taylor Model Basin Report 1393, January, 1961.

6 G. Gerard, "Compressive and Torsional Buckling of Thin-Wall Cylinders in Yield Region," National Advisory Committee for Aeronautics, Note 3726, August, 1956.

7 J. G. Pulos, and V. L. Salerno, "Axisymmetric Elastic Deformations and Stresses in a Ring-Stiffened, Perfectly Circular Cylindrical Shell Under External Hydrostatic Pressure," David Taylor Model Basin Report 1497, September, 1961.

8 M. A. Krenzke, and R. D. Short, Jr., "Graphical Method for Determining Stresses in Ring-Stiffened Cylinders Under External Hydrostatic Pressure," David Taylor Model Basin Report 1348, October, 1959.

9 J. A. Nott, "Investigation on the Influence of Stiffener Size on the Buckling Pressures of Circular Cylindrical Shells Under Hydrostatic Pressure," David Taylor Model Basin Report 1600, December, 1961.

10 G. Gerard, "Plastic Stability Theory of Stiffened Cylinders Under Hydrostatic Pressure," New York University Technical Report SM 61-13, October, 1961.

11 G. Gerard, and S. Wildhorn, "A Study of Poisson's Ratio in the Yield Region," National Advisory Committee for Aeronautics, Technical Note 2561, June, 1952.

12 M. E. Lunchick, and R. D. Short, Jr., "Behavior

of Cylinders with Initial Shell Deflections," *Journal of Applied Mechanics*, vol. 24, December, 1957, pp. 559–564.

13 M. A. Krenske, "Effect of Initial Deflections and Residual Welding Stresses on Elastic Behavior and Collapse Pressure of Stiffened Cylinders Subjected to External Hydrostatic Pressure," David Taylor Model Basin Report 1327, April, 1960.

14 F. B. Seely, and J. O. Smith, "Advanced Mechanics of Materials," New York, John Wiley and Sons, Inc., 1955, p. 81.

15 J. Kempner, and V. L. Salerno, "Analysis of Inelastic Behavior of Transversely Reinforced Cylindrical Shells Under Hydrostatic Pressure," Polytechnic Institute of Brooklyn Aeronautical Laboratory, Report No. 172, August, 1950.

INITIAL DISTRIBUTION

Copies

14   CHBUSHIPS
    2 Sci & Res Sec (442)
    1 Lab Mgt (320)
    3 Tech Info Br (335)
    1 Ships Res Br (341)
    1 Applied Sci Br (342)
    1 Prelim Des Br (420)
    1 Prelim Des Sec (421)
    1 Ship Protec (423)
    1 Hull Des Br (440)
    1 Struc Sec (443)
    1 Sub Br (525)

1   CHONR (439)

1   CNO (Op 07TB)

1   CDR, USNOL

1   CDR, USNRL (2027)

1   CDR, USNOTS, China Lake

1   CO, USNUOS

1   CO, USNUSL

10   CDR, ASTIA

2   NAVSHIPYD PTSMH

1   NAVSHIPYD MARE

1   NAVSHIPYD CHASN

2   NAVSHIPYD NY
    1 Matl Lab (948)

1   SUPSHIP, Groton

1   Elec Boat Div, Genl Dyn Corp

1   SUPSHIP, Newport News

1   NNSB & DD Co

1   SUPSHIP, Pascagoula

1   Ingalls Shipbldg Corp

1   DIR DEF R & E,
    Attn: Tech Lib

1   CO, USNROTC & NAVADMINU, MIT

1   O in C, PGSCOL, Webb

Copies

1   Dr. E. Wenk, Jr., The White House

1   Dr. R.C. De Hart, SW Res Inst

1   Prof. J. Kempner, Polytech Inst of Bklyn

1   Dean V.L. Salerno, Fairleigh Dickinson Univ

2   Dr. G. Gerard, College of Eng, New York Univ

David Taylor Model Basin. Report 1688.
   INVESTIGATION ON THE INFLUENCE OF STIFFENER SIZE ON THE BUCKLING PRESSURES OF CIRCULAR CYLINDRICAL SHELLS UNDER HYDROSTATIC PRESSURE, by James A. Nott. Jan 1963. ii, 11p. illus., tables, diagrs., refs. Reprinted from Journal of Ship Research, 6(2):24--32, Oct 1962.
   UNCLASSIFIED

   A theoretical derivation is given for elastic and plastic buckling of stiffened, circular cylindrical shells under uniform external hydrostatic pressures. The theory accounts for variable shell stresses, as influenced by the circular stiffeners, and critical buckling pressures are obtained for simple support conditions at the shell-frame junctures. Collapse pressures for both elastic and plastic buckling are determined by iteration and numerical minimization. The theory is applicable to shells

---

David Taylor Model Basin. Report 1688.
   INVESTIGATION ON THE INFLUENCE OF STIFFENER SIZE ON THE BUCKLING PRESSURES OF CIRCULAR CYLINDRICAL SHELLS UNDER HYDROSTATIC PRESSURE, by James A. Nott. Jan 1963. ii, 11p. illus., tables, diagrs., refs. Reprinted from Journal of Ship Research, 6(2):24--32, Oct 1962.
   UNCLASSIFIED

   A theoretical derivation is given for elastic and plastic buckling of stiffened, circular cylindrical shells under uniform external hydrostatic pressures. The theory accounts for variable shell stresses, as influenced by the circular stiffeners, and critical buckling pressures are obtained for simple support conditions at the shell-frame junctures. Collapse pressures for both elastic and plastic buckling are determined by iteration and numerical minimization. The theory is applicable to shells

---

David Taylor Model Basin. Report 1688.
   INVESTIGATION ON THE INFLUENCE OF STIFFENER SIZE ON THE BUCKLING PRESSURES OF CIRCULAR CYLINDRICAL SHELLS UNDER HYDROSTATIC PRESSURE, by James A. Nott. Jan 1963. ii, 11p. illus., tables, diagrs., refs. Reprinted from Journal of Ship Research, 6(2):24--32, Oct 1962.
   UNCLASSIFIED

   A theoretical derivation is given for elastic and plastic buckling of stiffened, circular cylindrical shells under uniform external hydrostatic pressures. The theory accounts for variable shell stresses, as influenced by the circular stiffeners, and critical buckling pressures are obtained for simple support conditions at the shell-frame junctures. Collapse pressures for both elastic and plastic buckling are determined by iteration and numerical minimization. The theory is applicable to shells

---

David Taylor Model Basin. Report 1688.
   INVESTIGATION ON THE INFLUENCE OF STIFFENER SIZE ON THE BUCKLING PRESSURES OF CIRCULAR CYLINDRICAL SHELLS UNDER HYDROSTATIC PRESSURE, by James A. Nott. Jan 1963. ii, 11p. illus., tables, diagrs., refs. Reprinted from Journal of Ship Research, 6(2):24--32, Oct 1962.
   UNCLASSIFIED

   A theoretical derivation is given for elastic and plastic buckling of stiffened, circular cylindrical shells under uniform external hydrostatic pressures. The theory accounts for variable shell stresses, as influenced by the circular stiffeners, and critical buckling pressures are obtained for simple support conditions at the shell-frame junctures. Collapse pressures for both elastic and plastic buckling are determined by iteration and numerical minimization. The theory is applicable to shells

made either of strain-hardening or elastic-perfectly plastic materials. Using the developed analysis, it is shown that a variation in stiffener size can change the buckling pressures. Test data from high-strength steel and aluminum cylinders show agreement between the theoretical and experimental collapse pressures to within approximately six percent.

made either of strain-hardening or elastic-perfectly plastic materials. Using the developed analysis, it is shown that a variation in stiffener size can change the buckling pressures. Test data from high-strength steel and aluminum cylinders show agreement between the theoretical and experimental collapse pressures to within approximately six percent.

made either of strain-hardening or elastic-perfectly plastic materials. Using the developed analysis, it is shown that a variation in stiffener size can change the buckling pressures. Test data from high-strength steel and aluminum cylinders show agreement between the theoretical and experimental collapse pressures to within approximately six percent.

made either of strain-hardening or elastic-perfectly plastic materials. Using the developed analysis, it is shown that a variation in stiffener size can change the buckling pressures. Test data from high-strength steel and aluminum cylinders show agreement between the theoretical and experimental collapse pressures to within approximately six percent.

made either of strain-hardening or elastic-perfectly plastic materials. Using the developed analysis, it is shown that a variation in stiffener size can change the buckling pressures. Test data from high-strength steel and aluminum cylinders show agreement between the theoretical and experimental collapse pressures to within approximately six percent.

made either of strain-hardening or elastic-perfectly plastic materials. Using the developed analysis, it is shown that a variation in stiffener size can change the buckling pressures. Test data from high-strength steel and aluminum cylinders show agreement between the theoretical and experimental collapse pressures to within approximately six percent.

made either of strain-hardening or elastic-perfectly plastic materials. Using the developed analysis, it is shown that a variation in stiffener size can change the buckling pressures. Test data from high-strength steel and aluminum cylinders show agreement between the theoretical and experimental collapse pressures to within approximately six percent.

made either of strain-hardening or elastic-perfectly plastic materials. Using the developed analysis, it is shown that a variation in stiffener size can change the buckling pressures. Test data from high-strength steel and aluminum cylinders show agreement between the theoretical and experimental collapse pressures to within approximately six percent.